Research Article

ADVANCED PHOTONICS

High-resolution and wide-field microscopic imaging with a monolithic meta-doublet under annular illumination

Jiacheng Sun,[a,b,†] Wenjing Shen,[a,†] Junyi Wang,[a,b,†] Rongtao Yu,[a,b] Jian Li,[a] Chunyu Huang,[a] Xin Ye,[a] Zhaoyu Cheng,[b] Jiefu Yu,[b] Peng Wang,[b] Chen Chen,[a,*] Shining Zhu,[a] and Tao Li[a,*]

[a]Nanjing University, College of Engineering and Applied Sciences, National Laboratory of Solid State Microstructures, Key Laboratory of Intelligent Optical Sensing and Manipulation, Jiangsu Key Laboratory of Artificial Functional Materials, Nanjing, China
[b]MetaCV Technology Co., Ltd., Nanjing, China

Abstract. Metalenses have exhibited significant promise across various applications due to their ultrathin, lightweight, and flat architecture, which allows for integration with microelectronic devices. However, their overall imaging capabilities, particularly in microscopy, are hindered by substantial off-axis aberrations that limit both the field of view (FOV) and resolution. To address these issues, we introduce a meta-microscope that utilizes a metalens doublet incorporated with annular illumination, enabling wide FOV and high-resolution imaging in a compact design. The metalens-doublet effectively mitigates off-axis aberrations, whereas annular illumination boosts resolution. To validate this design, we constructed and tested the meta-microscope system, attaining a record resolution of 310 nm (for metalens image) with a 150 μm FOV at 470 nm wavelength. Moreover, by utilizing the integration of metasurface, we implemented a compact prototype achieving an impressive 1-mm FOV with a resolution of 620 nm. Our experimental results demonstrate high-quality microscopic bio-images that are comparable to those obtained from traditional microscopes within a compact prototype, highlighting its potential applications in portable and convenient settings, such as biomedical imaging, mobile monitoring, and outdoor research.

Keywords: metalens-doublet; microscopic imaging; field of view; high resolution.

Received Feb. 11, 2025; revised manuscript received Apr. 8, 2025; accepted for publication Apr. 28, 2025; published online May 27, 2025.

[DOI: 10.1117/1.AP.7.4.046006]

1 Introduction

Metalenses enable precise control of light at sub-wavelength scales with a flat architecture.[1–3] Their compactness, lightweight, and flexibility, provide significant advantages for creating compact imaging platforms that can perform multiple functions through diverse meta-atom designs.[4–11] This makes them promising candidates for miniaturized optical devices such as meta-cameras, on-chip spectrometers, and endoscopes.[12–22] Metalens with an extremely high numerical aperture (NA) for focusing working in the visible region was also proposed.[23] However, the performance of metalenses, especially in microscopic imaging, still falls short of optimal standards. In microscopy, the primary metric for performance is resolution, followed by the effective field of view (FOV). Unfortunately, the resolution and FOV in current meta-microscopy systems remain inadequate.[24–33] It is widely recognized that there exists an inherent trade-off between imaging resolution and FOV, constrained by the limited space-bandwidth product (SBP).[34] Thus, enhancing resolution will inherently diminish the FOV, a challenge that is exacerbated in meta-microscope imaging. While some advancements have achieved sub-micron resolution, their FOV is extremely restricted. Furthermore, there often exists a significant disparity between the intended NA of metalenses and the actual resolution attained, particularly at high NA values, complicating efforts to enhance resolution

*Address all correspondence to Chen Chen, chenchen2021@nju.edu.cn; Tao Li, taoli@nju.edu.cn

†These authors contributed equally to this work.

solely by increasing the NA (see more details in Note 1 in the Supplementary Material).

In fact, inspired by traditional lens groups, stacking multiple metalenses would be a promising solution to expand the FOV in far-field imaging.[35–38] However, few of them were particularly designed for microscopy according to the severer requirement of high resolution, which is a major inadequacy compared with the traditional microscope. Recently, lensless imaging has brought significant advancements with compact imaging devices, but it heavily relies on computational post-processing, which can be resource-intensive and prone to artifacts.[39–41] Therefore, compact meta-microscopes with both high resolution and large FOV are still in increasingly high demand.

In this work, we propose an efficient approach to achieving both high resolution and a wide FOV with a metalens doublet incorporating an annular illumination, as schematically shown in Fig. 1. The system consists of a metalens doublet as the objective made of silicon nitride nano-fins, positioned on both sides of a silica substrate. As illuminated by annular oblique incidence, which is generated by a Köhler illumination path, the microscopy resolution is further enhanced due to the expansion of k-space in the microscopic imaging process. In this way, our metalens microscope is implemented with the objective NA of 0.5, achieving FOV of up to 150 μm, and a resolution of 310 nm, which is a word-record value, to our knowledge, far exceeding the highest one in reported meta-microscopy. Furthermore, by fully utilizing metasurfaces to achieve annular illumination, a highly compact prototype has been implemented (see inset of Fig. 1), where the microscopy FOV is further expanded to 1 mm with a resolution of 620 nm by slightly reducing the object NA to 0.3. Both of them, to our knowledge, have exceeded the largest SBP reported in meta-microscopy with similar objective diameters till now, showing the powerful capability in microscopic bio-imaging.

2 Materials and Methods

2.1 Design of Metalens Doublet

Figure 2(a) schematically illustrates the design of metalens-doublet, which is composed of metalens-I facing the object and metalens-II in the backside, with a separation distance determined by the substrate. According to the experiments, the substrate is defined as fused silica with a thickness of 500 μm, and the object plane is designed at 317 μm in front of the metalens-I, with respect to a three-fold magnification in the image plane. The phase profiles of both metalenses are optimized for a 150-μm FOV using the ray tracing method in Zemax OpticStudio, at an operating wavelength of 470 nm. The focal spots of the metalens doublet at the center and an object height of 75 μm are optimized at the realm of the FOV, which needs to be well confined within the Airy disk [see the red tracks in Fig. 2(a), where the black circle denotes the Airy disk boundary].

The phase profiles of the metalenses were chosen as follows:

$$\phi(r) = \sum_{n=1}^{10} a_n \left(\frac{r}{R}\right)^{2n}, \tag{1}$$

where R is the radius of the metalens, which equals 0.225 and 0.12 mm for metalens-I and metalens-II, respectively, and a_n is the optimized coefficient (see more details in Note 2 in the Supplementary Material). Figure 2(b) shows the phase profiles obtained by optimizing the focal spot with ray tracing. The metalens-I features a steep phase distribution (red), playing the major role of focusing, whereas the phase profile of metalens-II (blue) is relatively gentle [see the zoom-in figure in Fig. 2(b)], acting similarly to a phase corrector for the monochromatic aberrations. Actually, it works similar to a reversed configuration of previous metalens doublet for far-field wide-angle imaging.[35,36]

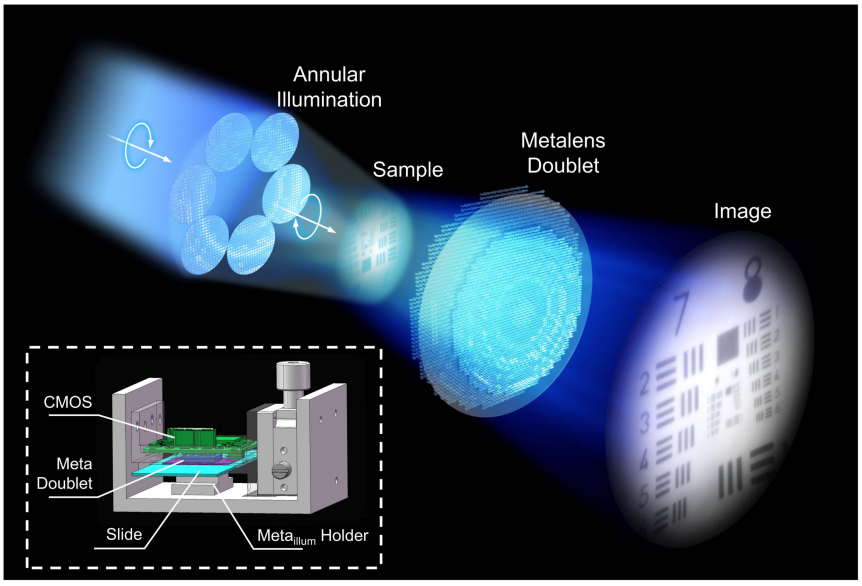

Fig. 1 Schematic of the meta-microscope based on metalens doublet and annular illumination. The optimized doublet enlarges the FOV and the annular illumination improves the resolution. Inset is the implemented meta-microscope prototype in a very compact form.

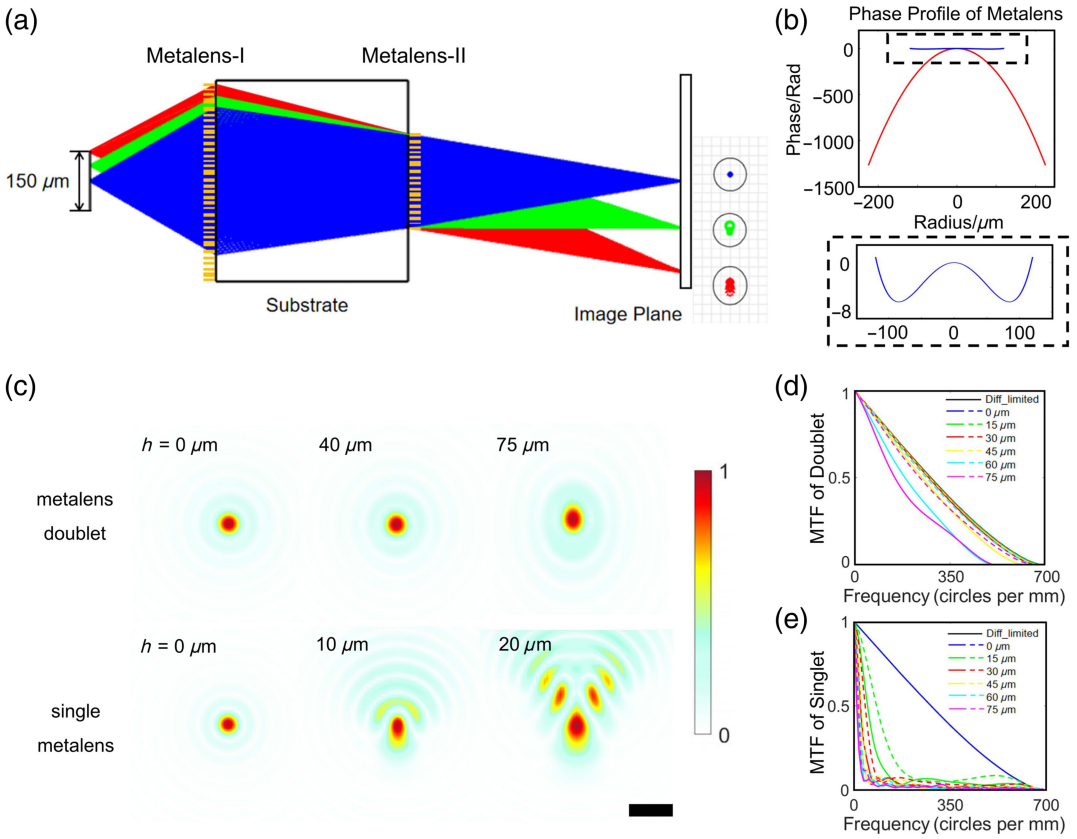

Fig. 2 Optical design of the metalens doublet. (a) Ray tracing simulation schematic diagram of the metalens doublet of 150 μm FOV at the working wavelength of 470 nm. The diameters of the metalens-I and metalens-II are 450 and 240 μm, located on both sides of a 500-μm-thick fused silica substrate. The blue, green, and red optical paths and spot diagrams correspond to object heights of 0, 40, and 75 μm, respectively. (b) The optimized phase profiles of the metalens-I (red) and metalens-II (blue). (c) Calculated PSFs of the metalens doublet at different object heights, with the PSFs of the single-layer metalens at varied object heights included at the bottom for comparison. Scale bar is 10 μm. Calculated MTFs of different object heights of (d) the metalens doublet and (e) single metalens, respectively.

By employing the optimized phase distribution, we computed the point spread function (PSF) at various focal points corresponding to different object heights through Rayleigh–Sommerfeld diffraction integration in MATLAB, illustrated in Fig. 2(c). The findings indicate that the metalens doublet achieves nearly diffraction-limited focusing for object heights reaching up to 75 μm from the center of the FOV. In contrast, the PSFs for a single-layer metalens with identical NA and diameter are displayed at the bottom of Fig. 2(c), revealing diffraction-limited focusing only for on-axis point object, with considerable aberrations present for small off-axis angles. The phase modulation of the singlet metalens is designed to be spherical-aberration free as $\varphi = -2\pi/\lambda(\sqrt{s^2 + r^2} + \sqrt{s'^2 + r^2})$, where λ, s, and s' are the working wavelength, object distance, and image distance, respectively. Furthermore, the related modulation transfer function (MTF) curves are depicted in Fig. 2(d), whereas the MTF curves for a single metalens are presented in Fig. 2(e). Both the PSF and MTF of the metalens doublet demonstrate superior imaging performance across a broad FOV, highlighting an excellent correction of monochromatic aberrations.

2.2 *Imaging Setup of Metalens Doublet and Annular Illumination*

To characterize the imaging performance of the metalens doublet, we designed, fabricated, and tested the doublet at the wavelength of 470 nm. Each nano-fin of the metalens is crafted as a high-aspect-ratio square with a fixed height of 1 μm and arranged at intervals of 300 nm considering the Nyquist-Shannon sampling theorem.[42] We chose SiN_x, which has a refractive index of 2.0 at 470 nm, for its low optical loss in the visible spectrum and compatibility with the complementary metal-oxide semiconductor (CMOS) fabrication techniques. The cross-sectional dimensions in nanometers (nm) of the 12 square nano-fins in the metalens-I are illustrated in Fig. 3(a), with their sizes (in nanometers) labeled along the phase distribution line. For metalens-II, the rectangular nano-fins have a length of 230 nm and a width of 90 nm, as illustrated in Fig. 3(b). In our design, we combine a propagation phase layer with a PB phase layer to induce a circular polarization change between the incident and outgoing light. This polarization control enables the effective filtering of light that does not contribute to our designed modulation using a circular polarization

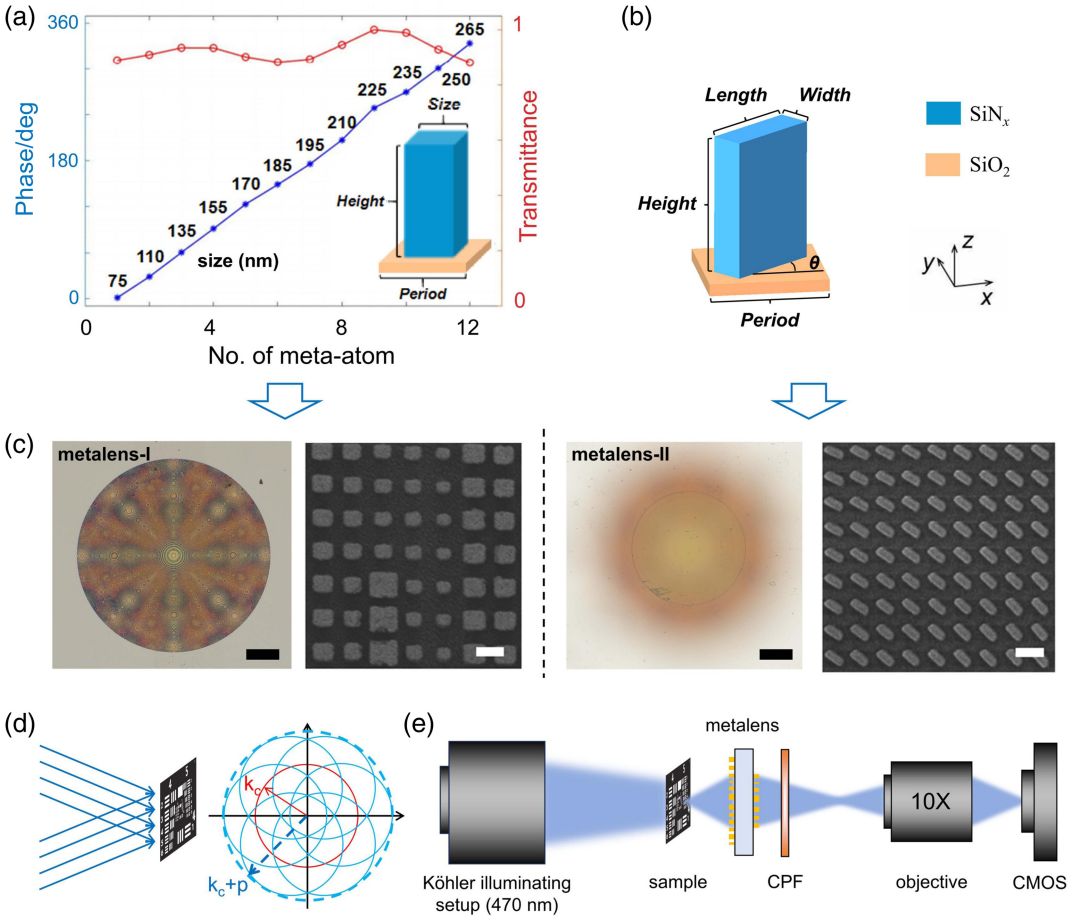

Fig. 3 Characterization of the metalens doublet. (a) Phase and transmittance of meta-atoms with 12 different structural parameters, simulated by FDTD solutions. The sizes (in nanometers) of the nano-fins are marked along the phase distribution line. (b) Schematic of a single unit cell, the width and length of the nano fins are 90 nm and 230 nm, respectively. (c) Optical and top-view scanning electron microscope (SEM) images of the fabricated SiN_x metalenses. Scale bar is 75 μm and 300 nm, respectively. (d) Annular oblique lighting can expand the spectrum pass-band so that high-frequency information can be received, thus improving the resolution. (e) Schematic drawing of the measurement setup.

filter (CPF), thereby improving the imaging system's signal-to-noise ratio. All of the metalenses were fabricated using standard electron-beam lithography and dry etching on a 1-μm-thick SiN_x film deposited on both sides of a fused silica substrate, which has a refractive index of 1.48 at 470 nm (see more details in Note 2 in the Supplementary Material). Figure 3(c) displays the optical images and top-view scanning electron microscope (SEM) images of the fabricated SiN_x metalens. Before employing annular illumination, we characterized the metalens doublet's microscopy imaging performance, analyzing its resolution, PSFs, MTFs, and Strehl ratios. These evaluations demonstrated high-quality imaging across the entire FOV, indicating excellent imaging capabilities (see more details in Note 3 in the Supplementary Material).

Following the basic characterization of the metalens doublet, the imaging capabilities of the meta-microscope are further examined in cooperation with the annular illumination system. As previously discussed, many studies on meta-microscopy encounter challenges in achieving a high resolution as designed with a large NA. This difficulty primarily arises from the steep increase in the phase gradient at the periphery of the metalens as the NA increases, leading to inadequate sampling frequency at the edges. Furthermore, the angular dispersion of sub-wavelength structures at the metalens edge becomes more pronounced with higher NA. Therefore, unlike traditional refractive lenses, the NA of metalenses cannot increase ideally with improved resolution as expected. This limitation is a key reason why the ultra-high resolution of meta-microscopy is rarely reported. Consequently, the effective FOV and resolution of most meta-microscope configurations tend to fall short of optimal performance, with SBP typically in the range of only 10^3 to 10^4.

Fortunately, the resolution of an imaging system is not exclusively determined by the lens's NA. Enhancing resolution by utilizing illumination to complement the NA is a promising strategy[43–45] (see more details in Note 4 in the Supplementary Material). When a sample is illuminated by normal plane waves, the zeroth-order diffracted light scattered by the sample is centered within the objective lens aperture. As a result, only the low-order diffracted light that enters the aperture ($|\boldsymbol{k}| < k_c$)

can be transmitted, which restricts the variety of spatial frequencies that can be collected from the object. By adjusting the angle of the incident plane wave to achieve oblique illumination, the diffraction angle of the zeroth-order light is altered correspondingly. In this setup, higher-order diffracted light, which carries high-frequency details of the object, can also be captured through the aperture of the objective lens. The degree of expansion in the pass-band is influenced by the magnitude of the transverse wave vector of the illuminating wave. Changing the direction of the incoming light enhances isotropic resolution in all directions, as depicted in Fig. 3(d), where k_c and p are initial and expansion of cut-off frequency, respectively. As a result, the equivalent NA that the system can actually achieve equals $\mathrm{NA_{obj}} + \mathrm{NA_{illum}}$.

In our experimental demonstrations, we built a Köhler illumination to provide annular illumination, consisting of an LED light source, three focusing lenses, and two apertures. The illumination NA was adjustable by modifying the field aperture size (see more details in Note 2 in the Supplementary Material). Leveraging this system, we introduced annular illumination to enhance resolution, as illustrated schematically in Fig. 3(e). In this setup, the Köhler illumination system provided tailored lighting for the sample, where $\mathrm{NA_{illum}} = 0.5$, and the metalens doublet and CMOS sensor handled imaging and data acquisition. Compared to normal illumination, the annular illumination system significantly improved resolution, demonstrating its effectiveness in pushing the boundaries of meta-microscopy.

3 Results

3.1 Imaging under Annular Illumination

We characterized the imaging performance of the meta-microscope system utilizing a 1951 United States Air Force (USAF) resolution test chart as the object. For comparison, we also fabricated and tested a single-layer, spherical-aberration-free metalens with the same aperture diameter and focal length. The results reveal that the singlet metalens produces significant

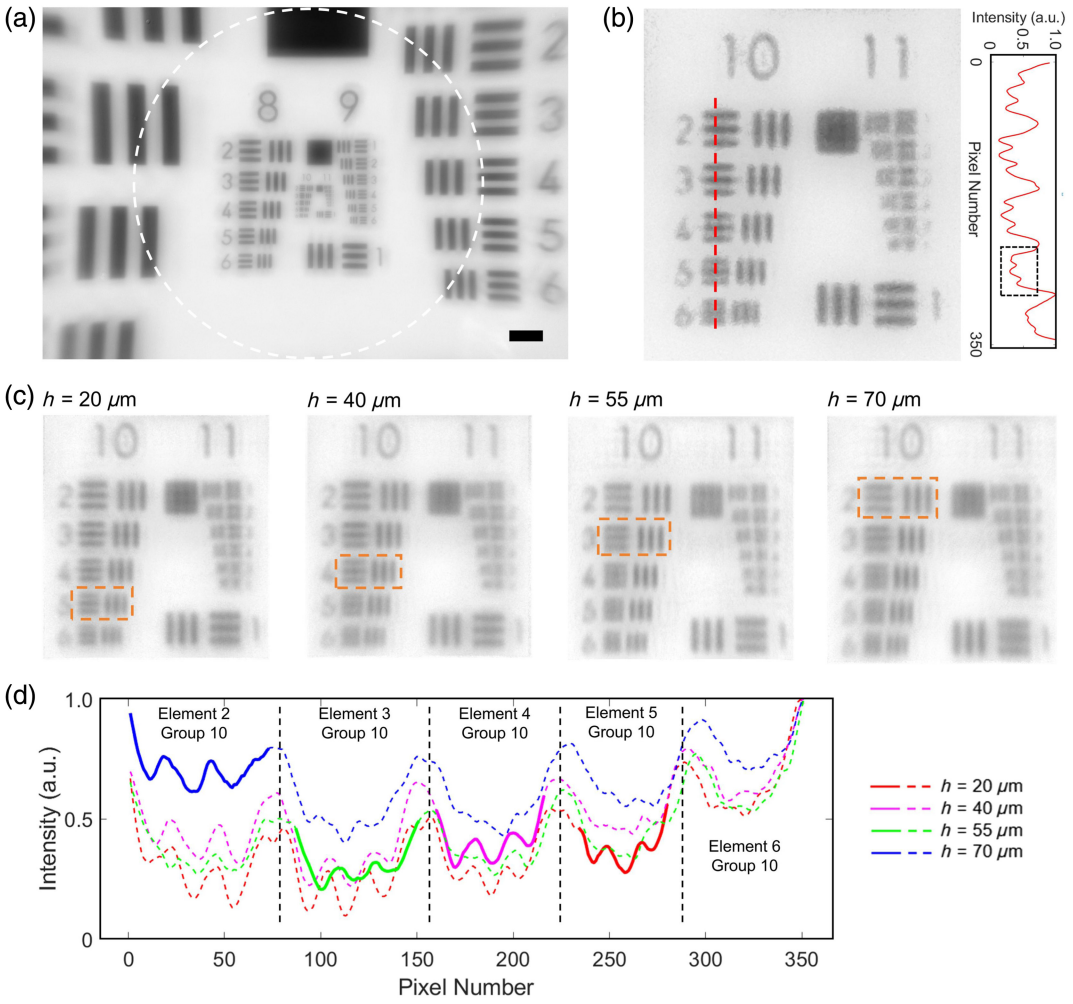

Fig. 4 Microscopic imaging performance. (a) Image of the whole FOV captured by the CMOS. Scale bar is 15 μm. (b) Image of resolution detail captured by the CMOS in the case of annular illumination. Element 5, group 10 can be recognized, indicating a resolution up to 310 nm. (c) Resolution characterization at object heights (i.e., distance from the optical axis) of 20, 40, 55, and 70 μm. (d) Normalized intensity profiles of the vertical line pairs corresponding to the achievable resolution, where the highest-resolution features are highlighted with solid curves.

blurriness at an object height of 20 μm and is nearly incapable of imaging at 55 μm. High-quality imaging is only achieved near the optical axis, with a limited FOV of ~20 μm in diameter (see more details in Note 5 in the Supplementary Material). By contrast, as shown in Fig. 4(a), the metalens doublet achieves high-clarity imaging across the entire designed FOV (outlined by the dashed circle), spanning 150 μm in diameter and covering an angular FOV of 27 deg with respect to the center of metalens-I. In addition, despite minor aberrations, some information outside the designed FOV can still be discerned.

More importantly, our meta-microscope system has achieved an unprecedented resolution. To date, there have been no prior reports of metalenses capable of resolving group 10 of the resolution chart. The detailed image of groups 10 and 11 is extracted to emphasize the resolution capabilities. As shown in Fig. 4(b), element 5, group 10 is resolvable from the imaging result and normalized intensity profiles of group 10, corresponding to a resolution of 310 nm. To be mentioned, the auxiliary objective lens used in the system does not influence the intrinsic resolution of the device, which is primarily determined by the object NA of the metalens doublet and the illumination condition. Furthermore, our meta-microscope system consistently demonstrates high resolution, exceeding element 2, group 10, across the entire FOV. To be more specific, we moved the resolution chart along the y-direction (parallel to the vertical line pairs) to capture the images of groups 10 and 11 at different object heights. Figures 4(c) and 4(d) display the resolution performance and normalized intensity profiles of vertical line pairs from group 10 at varying object heights, with the highest-resolution features highlighted [see the solid curve segments in Fig. 4(d)]. It is worth noting that the resolution in the horizontal direction remains uniformly high, whereas a slight decrease is

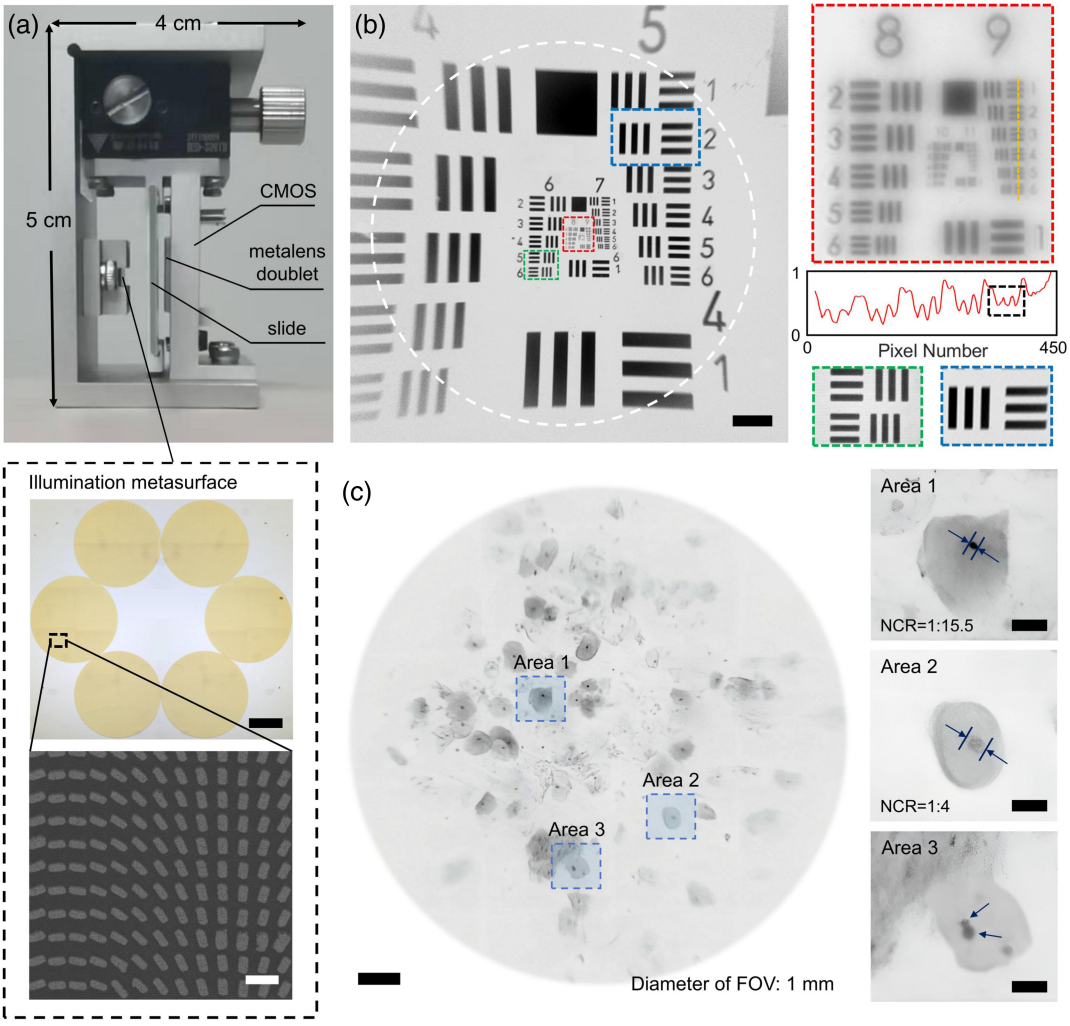

Fig. 5 Meta-microscope prototype and its application in bio-diagnostics. (a) Photographic image of the meta-microscope prototype, along with the optical and top-view SEM images of the fabricated illumination metasurface. Scale bar is 400 μm and 500 nm for the optical and SEM images, respectively. (b) Images of the USAF resolution test chart taken with the metalens microscope. Scale bar is 100 μm. (c) Images of the cervical cancer cells. Scale bar is 80 μm. Area 1: normal cell with nuclei approximately several micrometers in size. Area 2: pathological cell with significantly increased nuclear-cytoplasmic ratio. Area 3: pathological cell whose nuclei begin to divide. Scale bar is 10 μm for enlarged areas 1–3.

observed in the vertical direction. This decrease is acceptable for larger object heights and tilted fields of view, where the equivalent entrance pupil is elliptical and aligns with the characterization results of the PSFs and MTFs. Consequently, the SBP of our meta-microscope is calculated to be 5.8×10^5, which significantly surpasses that of previously reported meta-microscopes (see more details in Note 7 in the Supplementary Material).

3.2 Meta-microscope Prototype with an Large FOV

Although the above meta-microscope system design achieves an unprecedented combination of high resolution and a relatively large FOV, it remains more adaptable for general applications where a larger FOV is usually required. Even employing the double-layer metalens, the large effective NA of 0.5 still limits the effective FOV to hundreds of microns. To further demonstrate the flexibility and superiority of our approach, we designed and fabricated another compact meta-microscope prototype with the effective FOV expanding to a millimeter scale.

Based on the analysis in Note 1 in the Supplementary Material, we appropriately reduce the object NA to 0.3 and enlarge the aperture of lens-doublet, enabling a notable FOV of 1 mm in diameter with a corresponding angular FOV of 54 deg (measured from the center of metalens-I), and achieving a resolution of 620 nm. Leveraging the unique light manipulation capabilities of metasurfaces, we also designed an annular illumination system within a highly compact framework. This was accomplished by fabricating an illumination metasurface composed of six segments 1 mm away from the overall center, each configured to illuminate a 1-mm-diameter area from different directions. The fabrication process for the illumination metasurface is similar to that used for the metalens doublet. The phase modulation of each metasurface takes the form as $\varphi = -2\pi/\lambda \mathrm{NA}_{\mathrm{illum}}(\cos\,\phi x + \sin\,\phi y)$, where $\mathrm{NA}_{\mathrm{illum}} = \sin\,\theta$ with θ representing the illumination angle and ϕ is the azimuth angle. We developed a miniaturized prototype that integrates a CMOS sensor, CPFs, a metalens doublet, an illumination metasurface, and a sample holder. The entire device measures just 4 cm × 4 cm × 5 cm, achieving a 1000-fold reduction in size and weight compared to a bulky Olympus microscope. Figure 5(a) displays the internal structure of our device and highlights the fabricated metasurface for illumination. By combining the metasurface with PB phase design and CPFs, the system effectively removes unmodulated background light, ensuring that only illumination at the desired inclination angle (11.5 deg, corresponding to $\mathrm{NA}_{\mathrm{illum}} = 0.2$) reaches the sample, achieving uniform and precisely controllable lighting. We characterized the system using a USAF resolution chart. The captured images, displayed in Fig. 5(b), include zoomed-in stitched sections that demonstrate the resolution and details across various object heights. A normalized intensity profile of group 9 reveals that element 5 can be clearly resolved, corresponding to a resolution of 620 nm. The detailed performance of the fabricated metalens-doublet is presented in Note 6 in Supplementary Material.

Moreover, our meta-microscope showcases significant potential in life sciences due to its ability to maintain high resolution across a large FOV. To demonstrate its bio-imaging capabilities, we imaged cervical cancer cells, as shown in Fig. 5(c). Compared with a conventional single-layer, spherical-aberration-free metalens, the integration of the metalens doublet and illuminated metasurfaces significantly expands both resolution and FOV, allowing detailed observation of cellular lesions across a 1-mm range. The insets in areas 1–3 display various stages of cellular canceration within the same FOV. Normal cells exhibit relatively regular circular nuclei with a typical size of 1.8 μm in diameter, as seen in area 1. As cancer progresses, nuclei enlarge and deform. In areas 2 and 3, images of cells from the early stage of lesion development and severely affected cancer cells reveal distinct features such as the higher nuclear-cytoplasmic ratio (NCR, from less than 1:10 to 1:5–1:3) and nuclear division. These results highlight the practical usage of our microscope for biomedical diagnosis. High-resolution imaging combined with a large FOV can help medical professionals efficiently identify and analyze tissue lesions, providing critical insights for diagnostics and treatment planning.

4 Discussion and Conclusion

As previously analyzed, there is an inherent trade-off between the NA and FOV of a metalens. Although multi-layer metalenses can significantly reduce off-axis aberrations, their effectiveness in high-NA systems remains limited. As the NA increases, the sampling frequency at the periphery of a large-aperture metalens often falls short, and larger diffraction angles reduce modulation efficiency, compromising focusing ability and causing deviations between the designed and actual imaging resolution. This challenge has been extensively documented in meta-microscopy research.[46,47] To facilitate comparison, we summarize the key parameters from recent studies, with the main

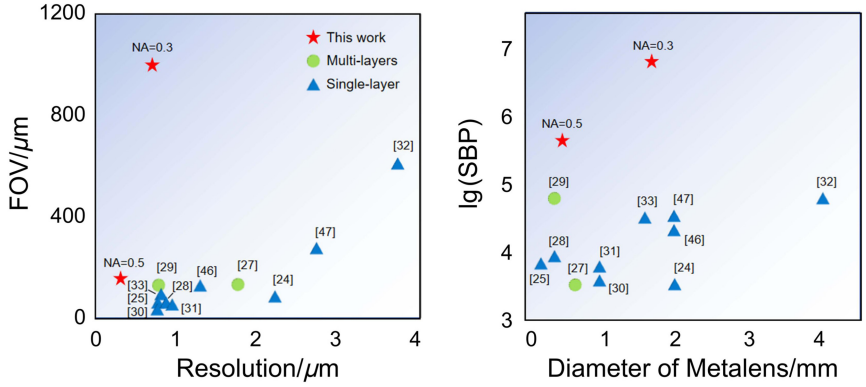

Fig. 6 Parameters and performance of some meta-based microscopes reported.

findings visually represented in Fig. 6 and detailed parameters provided in Note 7 in the Supplementary Material.

In this work, we developed a meta-microscopic imaging system that combines a SiN_x metalens doublet with annular illumination to achieve wide-field, high-resolution imaging. By carefully optimizing the meta-doublet design and annular illumination configuration, our meta-microscope demonstrated a record high resolution with relatively large FOV, showing overwhelming priority over previously reported data (see the red asterisks in Fig. 6 for the state-of-the-art comparison). Utilizing the integration of metasurface, a miniaturized metalens-based microscope can be constructed for *in vivo* diagnosis, which may allow to observe natural and human cells in real time and provide *in situ* biomedical observation across a wide FOV. These configurations were validated through both simulations and experiments and compared with a singlet metalens of equivalent NA and size. In the meantime, the SBPs of our meta-microscopes significantly surpassed those reported in similar works. Our approach combining meta-doublet with annular meta-illumination is applicable not only in compact microscopy but also opens a new avenue in designing other high-performance meta-devices and systems.

Disclosures

The authors declare no competing interests.

Code and Data Availability

Data underlying the results presented in this paper may be obtained from the authors upon reasonable request.

Acknowledgments

The authors acknowledge the Micro-fabrication Center of the National Laboratory of Solid State Microstructures (NLSSM) for technique support. The authors acknowledge financial support from the National Key Research and Development Program of China (Grant Nos. 2024YFA1012600 and 2022YFA1404301), National Natural Science Foundation of China (Grant Nos. 62325504, 62305149, 92250304, and 62288101), and Dengfeng Project B of Nanjing University.

References

1. N. Yu et al., "Light propagation with phase discontinuities: generalized laws of reflection and refraction," *Science* **334**, 333–337 (2011).
2. W. T. Chen, A. Y. Zhu, and F. Capasso, "Flat optics with dispersionengineered metasurfaces," *Nat. Rev. Mater.* **5**, 604–620 (2020).
3. T. Li et al., "Revolutionary meta-imaging: from superlens to metalens," *Photonics Insights* **2**, R01 (2023).
4. L. L. Huang et al., "Dispersionless phase discontinuities for controlling light propagation," *Nano Lett.* **12**, 5750–5755 (2012).
5. S. Sun et al., "High-efficiency broadband anomalous reflection by gradient meta-surfaces," *Nano Lett.* **12**, 6223–6229 (2012).
6. N. F. Yu and F. Capasso, "Flat optics with designer metasurfaces," *Nat. Mater.* **13**, 139–150 (2014).
7. A. Arbabi et al., "Dielectric metasurfaces for complete control of phase and polarization with subwavelength spatial resolution and high transmission," *Nat. Nanotechnol.* **10**, 937–943 (2015).
8. S. M. Kamali et al., "A review of dielectric optical metasurfaces for wavefront control," *Nanophotonics* **7**, 1041–1068 (2018).
9. H. Wang et al., "Independent phase manipulation of co- and cross-polarizations with all-dielectric metasurface," *Chin. Opt. Lett.* **19**, 053601 (2021).
10. J. Li et al., "Dual-band independent phase control based on high efficiency metasurface," *Chin. Opt. Lett.* **19**, 100501 (2021).
11. C. Chen et al., "Metasurfaces with planar chiral meta-atoms for spin light manipulation," *Nano Lett.* **21**, 1815–1821 (2021).
12. M. Khorasaninejad and F. Capasso, "Metalenses: versatile multifunctional photonic components," *Science* **358**, eaam8100 (2017).
13. M. S. Faraji-Dana et al., "Compact folded metasurface spectrometer," *Nat. Commun.* **9**, 4196 (2018).
14. E. Arbabi et al., "Full-Stokes imaging polarimetry using dielectric metasurfaces," *ACS Photonics* **5**, 3132–3140 (2018).
15. Y. Zhou et al., "Flat optics for image differentiation," *Nat. Photonics* **14**, 316–323 (2020).
16. C. Chen et al., "Highly efficient metasurface quarter-wave plate with wave front engineering," *Adv. Photonics Res.* **2**, 2000154 (2021).
17. M. Miyata et al., "Full-color-sorting metalenses for high-sensitivity image sensors," *Optica* **8**, 1596–1604 (2021).
18. J. Ji et al., "On-chip multifunctional metasurfaces with full-parametric multiplexed Jones matrix," *Nat. Commun.* **15**, 8271 (2024).
19. C. Chen et al., "Spectral tomographic imaging with aplanatic metalens," *Light Sci. Appl.* **8**, 99 (2019).
20. X. Ye et al., "Chip-scale metalens microscope for wide-field and depth-of-field imaging," *Adv. Photonics* **4**, 046006 (2022).
21. J. Chen et al., "Planar wide-angle-imaging camera enabled by metalens array," *Optica* **9**, 431–437 (2022).
22. J. Ji et al., "High-dimensional Poincaré beams generated through cascaded metasurfaces for high-security optical encryption," *PhotoniX* **5**, 13 (2024).
23. H. W. Liang et al., "Ultrahigh numerical aperture metalens at visible wavelengths," *Nano Lett.* **18**, 4460–4466 (2018).
24. L. Li et al., "Single-shot deterministic complex amplitude imaging with a single-layer metalens," *Sci. Adv.* **10**, eadl0501 (2024).
25. X. Wang et al., "Single-shot isotropic differential interference contrast microscopy," *Nat. Commun.* **14**, 2063 (2023).
26. Y. Luo et al., "Varifocal metalens for optical sectioning fluorescence microscopy," *Nano Lett.* **21**, 5133–5142 (2021).
27. H. Kwon et al., "Single-shot quantitative phase gradient microscopy using a system of multifunctional metasurfaces," *Nat. Photonics* **14**, 109–114 (2020).
28. Y. Long et al., "Metalens-based stereoscopic microscope," *Photonics Res.* **10**, 1501–1508 (2022).
29. Y. Liu et al., "Meta-objective with sub-micrometer resolution for microendoscopes," *Photonics Res.* **9**, 106–115 (2021).
30. Y. Kim et al., "Spiral metalens for phase contrast imaging," *Adv. Funct. Mater.* **32**, 2106050 (2022).
31. C. Wang et al., "Miniature two-photon microscopic imaging using dielectric metalens," *Nano Lett.* **23**, 8256–8263 (2023).
32. C. Sun et al., "Near-infrared metalens empowered dual-mode high resolution and large FOV microscope," *Adv. Opt. Mater.* **12**, 00512 (2024).
33. E. Arbabi et al., "Two-photon microscopy with a double-wavelength metasurface objective lens," *Nano Lett.* **18**, 4943–4948 (2018).
34. J. Park et al., "Review of bio-optical imaging systems with a high space-bandwidth product," *Adv. Photonics* **3**, 044001 (2021).
35. A. Arbabi et al., "Miniature optical planar camera based on a wide-angle metasurface doublet corrected for monochromatic aberrations," *Nat. Commun.* **7**, 13682 (2016).
36. B. Groever, W. T. Chen, and F. Capasso, "Meta-lens doublet in the visible region," *Nano Lett.* **17**, 4902–4907 (2017).
37. X. G. Luo et al., "Recent advances of wide-angle metalenses: principle, design, and applications," *Nanophotonics* **11**, 1–20 (2021).
38. F. Yang et al., "Wide field-of-view metalens: a tutorial," *Adv. Photonics* **5**, 033001 (2023).
39. G. Jin et al., "Lens-free shadow image based high-throughput continuous cell monitoring technique," *Biosens. Bioelectron.* **38**, 126–131 (2012).

40. A. C. Sobieranski et al., "Portable lensless wide-field microscopy imaging platform based on digital inline holography and multi-frame pixel super-resolution," *Light Sci. Appl.* **4**, e346 (2015).
41. A. Ozcan and E. McLeod, "Lensless imaging and sensing," *Annu. Rev. Biomed. Eng.* **18**, 77–102 (2016).
42. J. W. Goodman, *Introduction to Fourier Optics*, 3rd ed., Roberts and Co. Publishers (2005).
43. J. Ruiz-Santaquiteria et al., "Low-cost oblique illumination: an image quality assessment," *J. Biomed. Opt.* **23**, 016001 (2018).
44. C. Sanchez et al., "Oblique illumination in microscopy: a quantitative evaluation," *Micron* **11**, 006 (2018).
45. B. Chen et al., "Resolution doubling in light-sheet microscopy via oblique plane structured illumination," *Nat. Methods* **19**, 1419–1426 (2022).
46. J. Wang et al., "Quantitative phase imaging with a compact meta-microscope," *NPJ Nanophotonics* **1**, 00007 (2024).
47. C. H. Chu et al., "Intelligent phase contrast meta-microscope system," *Nano Lett.* **23**, 11630–11637 (2023).

Jiacheng Sun received his bachelor's degree in physics from Nanjing University. He is currently a PhD candidate at the College of Engineering and Applied Science, Nanjing University. His research interest includes meta-based microscopy, integrated imaging devices, and advanced compound fabrication process.

Chen Chen obtained her bachelor's and PhD degrees from Nanjing University in 2016 and 2021, respectively. Her research interest includes meta-photonics, metalens imaging technology, and polarization optics. To date, she has published over 30 papers in journals including *Light Science & Applications*, *Optica*, *Physical Review Letters*, *Nano Letters*, and *PhotoniX*, with more than 1300 citations.

Tao Li is a professor at the College of Engineering and Applied Sciences at Nanjing University. He received his PhD from Nanjing University in 2005. His research interest includes optical metamaterials, topological photonics, and on-chip photonic integrations.

Biographies of the other authors are not available.